STUDY OF TURBULENT WAKE FLOWS IN CURVED DUCTS

H. A. Abdalla

Department of Mechanical Power Engineering, Faculty of Engineering,
Menoufia University, Shebin El-Kom, Egypt

ABSTRACT

Development of steady wake flows downstream of a wake generator such as a stationary circular cylinder and a symmetrical airfoil within curved pipes are investigated. The wake generator was installed normal to the plane of curvature. The wake characteristics behind the cylinder was varied using cylinders with different diameters, namely d/D = 0.1, 0.3 and 0.5. In the case of a wake behind an airfoil, the wake was subjected to a pressure gradient by placing the airfoil at different incidence angles, α = 0, 10 and 30 degrees. The effects of the wake behind a cylinder or airfoil upon the performance of curved pipes, which measured by the streamwise pressure loss, and the static pressure distributions along the pipe walls are investigated experimentally. Experimental data of curved pipes with two curvature ratios at different Reynolds number are presented. The velocity profile behind the wake generator is measured to find the wake characteristics such as the velocity defect and the half-wake width. It is concluded that, the minimum streamwise pressure loss coefficient of curved pipes strongly depends on the wake characteristics, the curvature ratio and the Reynolds number. The calculated results of the wake velocity defect, wake velocity profile and the half-wake width are obtained by solving the conservation of mass and momentum equations along with the k-ε turbulence model. The results show that, asymmetry in velocity profiles about the wake centerline is due to the pressure gradient and the curvature effects. The comparison between the measured and predicted data indicates that the steady wake flow is well predicted.

Keywords: Turbulent flow, Wake characteristics, Curved ducts, Loss coefficient, Turbulence model

INTRODUCTION

Curved ducts are widely used in many engineering applications such as piping systems, aircraft intakes, refrigeration, air conditioning and turbomachines. Flow through curved ducts are characterized by secondary flow effects caused by centrifugal forces acting normal to the flow. These influence the flow structure and consequently the pressure loss in a curved duct. For turbulent flow, the pressure distributions and the corresponding pressure losses are comparatively well documented for a wide range of Reynolds number, turning angle and curvature ratio, see for example Ito [1]. An extensive work for the generation of secondary flow is given by

Berger *et. al.* [2]. The effects of curvature ratio, downstream tangent length and Reynolds number on flow characteristics in 90 degrees bend were studied theoretically and experimentally by Abdalla, *et al.* [3]. They reported that, reducing the downstream tangent length and increasing the curvature ratio enhances the pressure loss along the bend.

The literature on zero-streamwise pressure gradient straight wakes includes those given by Schlichting [4], Townsend [5], Sreenivasan and Narasimha [6] and Wygnanski *et al.* [7]. They found that the far wake is self-preserving as far as the mean velocity is concerned but lacks the universality of the turbulent structure.

Gartshore [8] investigated the effect of pressure gradient on the decay of two-dimensional symmetrical wakes. Turbomachinery wake flow is an important case of turbulent flow with streamline curvature and pressure gradient effects. The curvature and pressure gradient will significantly affect the mean velocities and turbulent properties of the wake. Raj and Lakshminarayana [9] investigated the near and far wake characteristics of a cascade of airfoils for three different incidence angles. They reported the measurements of mean velocity, turbulence intensity and Reynolds stress. They showed asymmetric distribution and the decay of the wake defect was strongly dependent on the downstream variation of wake edge velocity. The effect of pressure gradient and curvature on wakes were investigated by Savil [10], Nakayama [11] and by Ramjee *et. al.* [12]. Savil investigated a fully developed cylinder wake that is abruptly turned 90 degrees by means of a back plate so that the wake is subjected to strong curvature and streamwise pressure gradient. The data for mean velocity and turbulent stress revealed the strong influence of curvature on the wake. The turbulent stresses fields are complex owing to the coexistence of the stabilized and destabilized regions across the wake and strong interaction between them. Nakayama [11] and Ramjee *et al.* [12] reported that the wake subjected to mild curvature and mild pressure gradient by deflecting it by an airfoil-like thin plate placed at small angles in the external flow. The measured data indicated a strong sensitivity of turbulence quantities, especially the Reynolds shear stress, to the curvature and pressure gradient. Recently, Schobeiri *et al.* [13] investigated theoretically and experimentally the development of steady and unsteady wake flows downstream of a stationary cylinder and the cylinders of a rotating wake generator in a curved channel at zero longitudinal pressure gradient. Measurements of mean velocity and turbulent shear stresses were conducted. Schobeiri and John [14] studied the wake development behind a stationary cylinder in a curved channel at positive longitudinal pressure gradient. Their results showed strong asymmetry in velocity and Reynolds stress components. The Reynolds stress components have higher values at the inner half of the wake than at the outer half of the wake. Comparison of the wake development in the curved channel between zero and positive pressure gradient showed that the decay of the velocity defect is faster at zero streamwise pressure gradient than at a positive pressure gradient. The growth of wake width is faster for a positive streamwise pressure gradient.

Studies of turbulent wake flow in a curved duct are much fewer in number as compared to those in a straight duct. This paper examines the effect of curved wakes associated with airfoil at angle of attack or a stationary circular cylinder on the performance of curved pipes. The effects of curvature ratio and Reynolds number are considered. Computations based on the k-ε model are performed to obtain more information about the curved wake development behind an airfoil or a cylinder in curved pipes.

NUMERICAL MODEL AND COMPUTATION PROCEDURE
The Governing Equations

The turbulence Reynolds equations for conservation of mass, momentum, turbulence energy, k, and its dissipation rate, ε, which govern the two-dimensional, incompressible, isothermal, steady and turbulent flows in curved ducts with upstream and downstream straight tangents, can be written for straight ducts, Cartesian coordinates system (z, y directions), as well as curved ducts, cylindrical coordinates system (θ,r directions); in the following general form, Reference 15:

$$\frac{1}{y^j}\frac{\partial}{\partial y}(\rho\, y^j\, v\, \Phi) + \frac{1}{y^j}\frac{\partial}{\partial \theta}(\rho\, u\, \Phi) =$$
$$\frac{1}{y^j}\frac{\partial}{\partial y}\left(\Gamma_\Phi\, y^j\frac{\partial \Phi}{\partial y}\right) + \frac{1}{y^j}\frac{\partial}{\partial \theta}\left(\Gamma_\Phi\,\frac{\partial \Phi}{y^j\,\partial \theta}\right) + S_\Phi \qquad (1)$$

where Φ is a depended variable (representing 1, u, v, k and ε for conservation of mass, u-momentum, v-momentum, turbulence energy and its dissipation rate, respectively, Γ_Φ is the exchange coefficient, and S_Φ represents the source term. Both Γ_Φ and S_Φ are replaced with suitable terms corresponding to the form Φ takes and are given in Table 1, where certain quantities are defined as follows:

$$G = \mu_t \left[2\left(\frac{1}{y^j}\frac{\partial u}{\partial \theta} + \frac{jv}{y^j}\right)^2 + 2\left(\frac{\partial v}{\partial y}\right)^2 + \left(\frac{1}{y^j}\frac{\partial v}{\partial \theta} + \frac{\partial u}{\partial y} - j\frac{u}{y^j}\right)^2 \right] \quad (2)$$

$$\mu_{eff} = \mu_\ell + C_\mu \rho \frac{k^2}{\varepsilon} \quad (3)$$

Table 1 Source Term in the General Equation for Φ, Equation 1

Conservation of	Φ	Γ_Φ	S_Φ
Continuity	1	0	0
Radial Momentum	v	μ_{eff}	$-\frac{\partial P}{\partial y} + \frac{1}{y^j}\frac{\partial}{\partial y}\left(\mu_t y^j \frac{\partial v}{\partial y}\right) + \frac{1}{y^j}\frac{\partial}{\partial \theta}\left(\mu_t(\frac{\partial u}{\partial y} - j\frac{u}{y^j})\right)$ $+ j\left(\frac{\rho u^2}{y^j} - \frac{\mu_{eff}}{y^j}(2\frac{\partial u}{y^j \partial \theta} + \frac{v}{y^j}) - \mu_t \frac{v}{y^{2j}}\right)$
Axial Momentum	u	μ_{eff}	$-\frac{1}{y^j}\frac{\partial P}{\partial \theta} + \frac{\partial}{\partial y}\left(\mu_t(\frac{\partial v}{y^j \partial \theta} - j\frac{u}{y^j})\right) + \frac{1}{y^j}\frac{\partial}{\partial \theta}\left(\mu_t(\frac{\partial u}{y^j \partial \theta} + j\frac{2v}{y^j})\right)$ $+ j\left(\frac{\mu_{eff}}{y^j}(2\frac{\partial v}{y^j \partial \theta} - \frac{u}{y^j}) - \frac{\rho u v}{y^j} + \frac{\mu_t}{y^j}(\frac{\partial u}{\partial y} - \frac{u}{y^j})\right)$
Turbulent Kinetic Energy	k	$\dfrac{\mu_{eff}}{\sigma_k}$	$G - C_D \rho \varepsilon$
Dissipation Rate of k	ε	$\dfrac{\mu_{eff}}{\sigma\varepsilon}$	$\frac{\varepsilon}{k}(C_1 G - C_2 \rho \varepsilon)$

where
j = 1 applied to curved duct,
j = 0 applied to straight tangent ducts

The standard constants necessary for the turbulence-model are given by Launder and Spalding [16] in Table 2.

Table 2 The standard Experimental Constants of k- ε Turbulence Model [16]

C_1	C_2	σ_k	σ_ε	C_D	C_μ
1.44	1.92	1.00	1.30	1.00	0.09

Houdeville and Tulapurkara [17] found that k-ε model of turbulence satisfactorily predicts the near-wake regions of symmetric and unsymmetric straight wakes. The effect of streamline curvature has been accounted for by modifying the value of the constant C_μ on similar lines discussed by Leschziner and Rodi [18]. The modified value of C_μ in the present work could be expressed as:

$$C_\mu = 0.09 \left/ \left[1 + 0.57 j \frac{k^2}{\varepsilon^2}\left(\frac{\partial u}{\partial y} + \frac{u}{y^j}\right)\frac{u}{y^j} \right] \right. \quad (4)$$

The solution procedure which uses the finite difference method to solve Equation 1 for variable Φ, is a development of Gosman and Pun's [19]. Briefly, by integrating the differential equations over grid cells, Figure 1, finite difference-equations are obtained for the two velocities u and v as well as for k

and ε. These equations are solved iteratively together with a pressure correction equation which known as [19]:

$$P = P^* + P'$$ (5)

where P^* is the guessed pressure at the starting of solution and P' is called the pressure correction. This equation modifies the pressure filed so that the converged solution also satisfies the continuity equation. More details about the solution procedure can be found in Ref. [19]. Converged solution were accepted when all normalized residuals were less than 0.005. The present computation was carried out with a finite difference mesh of 67 nodes in the streamwise direction and 29 nodes in normal direction. The calculation mesh and grid elements are shown in Figure 1 with unequally spaced grid nodes for improving the accuracy. Computations were made over the circular-cross section in the plane of curvature and started at a position five diameters upstream of the bend.

Figure 1 Computational domain of curved duct

Boundary Conditions

There are three different types of boundary conditions to specify for the computational domain shown in Figure 1. Inlet, outlet and wall boundary conditions. At the inlet, the following velocity distribution in the wake flow behind an airfoil presented by Schlichting [4] is used,

$$\frac{w}{w_0} = \left\{ 1 - 0.293 \, (y / \bar{b})^{3/2} \right\}^2$$ (6)

where $w = (U_0 - u)$ is the velocity defect, w_0 is its value at the wake center, $\bar{b}$ is the average value of the half-wake widths on the inner and outer walls of the curved duct and U_0 is the inlet velocity of the main flow. With the initial values of w_0 and $\bar{b}$, the inlet velocity distribution in the wake flow behind the airfoil can be generated using equation (6). In the case of a wake flow behind a circular cylinder, the following equation presented by Schlichting [4] is assumed to generate the inlet velocity profile,

$$\frac{w}{U_0} = 0.98 \, (d \, C_d / z)^{0.5} \left\{ 1 - (y / \bar{b})^{3/2} \right\}^2$$ (7)

where C_d is the drag coefficient of a circular cylinder placed in a uniform flow, d is the cylinder diameter and z is the streamwise distance measured from the cylinder position.

The normal velocity (v) is obtained by taking $v = 0$ at the centerline of the duct and then integrating the continuity equation. Knowing u as a function of y, the distribution of the inlet turbulence kinetic energy (k_{in}) is calculated according to Reference 20 as :

$$k_{in} = \ell \left(\frac{\partial u}{\partial y} \right)^2 / C_\mu^{1/2}$$ (8)

where ℓ is the mixing length and estimated as $\ell = 0.25 \, \bar{b}$. It may be remarked previously that in the central portion of the wake $\partial u / \partial y$ is small and becomes zero at the center. However, the turbulence kinetic energy in the central portion of the wake is
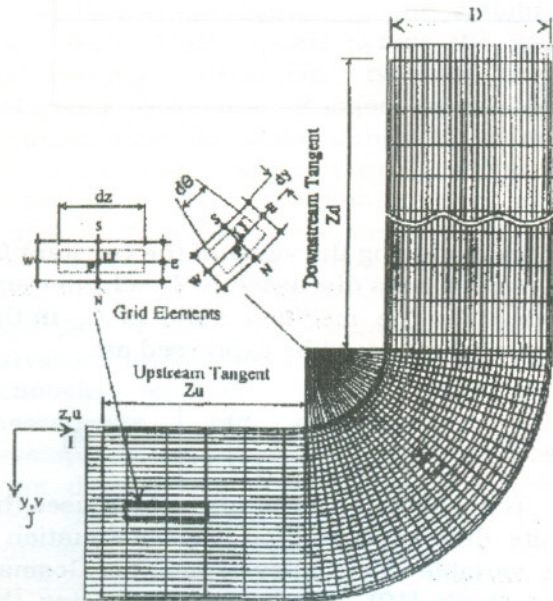
not much smaller than its maximum value as presented by Ramaprian et al. [20]. Hence, the turbulence kinetic energy is evaluated starting from the edges of the wake and using Equation 8 until its maximum value is attained. In the central region of the wake, turbulence kinetic energy is kept constant at its maximum value. The inlet profile of dissipation of turbulence kinetic energy (ε_{in}) is obtained from the following equation,

$$\varepsilon_{in} = C_\mu^{0.75} k^{1.5} / \ell \qquad (9)$$

At the outlet, gradient of flow variables in the flow direction are zero; $\frac{\partial \Phi}{\partial z} = 0$ (Neuman conditions), except the radial velocity v which is sit to zero. At the solid wall boundaries, however, u = v = 0., i.e. no-slip conditions. The near wall velocity, u_p (parallel to wall boundaries at a distance y_p) is determined by the logarithmic-law of the wall equation :

$$\frac{u_p}{u_\tau} = \frac{1}{\chi} \ell n (Ey_p^+) \qquad (10)$$

where u_τ and y_p^+ are the friction velocity and the dimensionless wall distance defined respectively by

$$u_\tau = \sqrt{\frac{\tau_w}{\rho}} \quad \text{and} \quad y_p^+ = \frac{\rho y_p u_\tau}{\mu_\ell} \qquad (11)$$

where τ_w is the wall shear stress, χ and E are the Von-Karmn's constant and the roughness parameter given by Reference 4 as $\chi = 0.42$ and E= 9.7 . On a similar line of Reference 16, in the range of local equilibrium, near walls leads to:

$$u_\tau = C_\mu^{0.25} \sqrt{k} \qquad (12)$$

$$\tau_w = \frac{\rho C_\mu^{0.25} \sqrt{k}}{\ell n (E y_p^+)/\chi} u_p \qquad (13)$$

$$\varepsilon_p = \frac{C_\mu^{0.25} k_p^{1.5}}{\chi y_p} \left[1 - j\frac{y_p}{y^j} \ell n (E y_p^+) \right]_p \qquad (14)$$

Equations 12 to 14 give the values of k and ε at the nearest wall point (p) without solving the transport equations. More details of the discretization, the solution procedure and boundary conditions were described previously by Abdalla, et al. [3].

EXPERIMENTAL RESEARCH FACILITY

A sketch of the test section is shown in Figure 2. Two screw compressors supply air at rate of 0.054 m³/s of air for each compressor. The air flows through a settling pipe, wake generating section and to then test section. Two bends with circular cross-section were made up of 90 degrees turning angle and with mean radius of curvature (R_c) of 136 mm and 260 mm, i.e. the curvature ratio ($\delta=D/2Rc$) is 0.37 and 0.216, respectively. All pipes are made of mild steel. The curved pipes of inside diameter (D) of 100 mm. The pressure taps with 1.0 mm inner diameter were drilled along the inner and outer walls of the bends in the plane of curvature. The test section was attached by a downstream tangent with 10 diameters in length.

In the present experiments, The NACA-0012 airfoil or a stationary circular cylinder was used as a wake generator, see Figure 2. The wake generator is installed vertically with its axis normal to the flow direction at a distance 150 mm (1.5 D) upstream the entrance to the curved test section. Therefore, the wake developed in the straight pipe and then subjected to a longitudinally curved flow. The airfoil used as a wake generator has a chord length of 100 mm and a span of 100 mm. The two-dimensional performance curves of the NACA-0012 airfoil were obtained from Reference 21. It is noted from the performance curves that, the stall angle of the flow over the airfoil is about 10 degrees. Trip wires with 1.0 mm diameter are placed at 0.2 chord from the leading edge of the airfoil so that the boundary layer at the trailing edge is turbulent. The wake is

subjected to pressure gradient and curvature by deflecting it by placing the airfoil at different setting angles with the flow direction, namely α = 0, 15 and 30 degrees, as shown in Figure 2. Then, in the upstream tangent the air was turned toward the streamwise direction as it entered the curved duct. For wake-producing cylinder, the wake strength was increased using circular cylinders with diameter ratios of d/D = 0.1, 0.3 and 0.5.
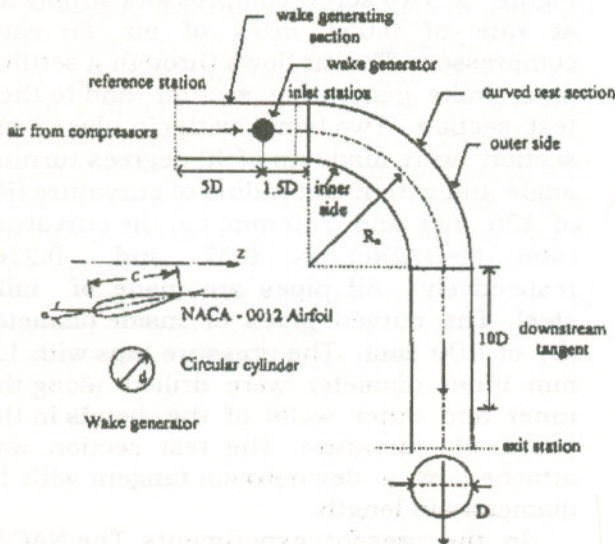

Figure 2 Layout of the test section

To determine the effects of the wake flow upon the pressure loss coefficient of bends, the pressure distributions along the inner and outer walls were measured with and without wake flow. The experiments were conducted for different Reynolds numbers and the pressure loss coefficients (K_b) were obtained. The mean inlet velocity profile at the bend entrance was measured at Reynolds number of 2.97×10^5 in the presence of the wake generator. The measurements of inlet velocity profiles were conducted for zero-incidence angle of airfoil and for cylinder diameter ratio of 0.5 using a calibrated three holes probe. The uncertainties of the measurements of the velocity profiles are estimated to be about 2 percent. The experimental errors in the

pressure measurements and the pressure loss coefficient are estimated to be about 1.2 and 3 percent, respectively.

EXPERIMENTAL RESULTS AND DISCUSSION
Wake Inlet Velocity Profiles

Measurements of the velocity profile at the entrance of the bend with a curvature ratio of 0.216 were conducted for analysis purpose. The measured wake velocity profiles behind NACA-0012 airfoil and a stationary circular cylinder of diameter 50 mm are presented in Figure 3. Velocity profiles are presented at Reynolds number of 2.97×10^5 based on a reference velocity of 43 m/s, measured at a distance 5D ahead the wake generator. It is seen from this figure that the velocity profiles in the near-wake region are asymmetrical. This is confirmed with the previous published data [12,13]. This asymmetric behavior is a result of the existing lateral pressure gradient generated by the curvature.
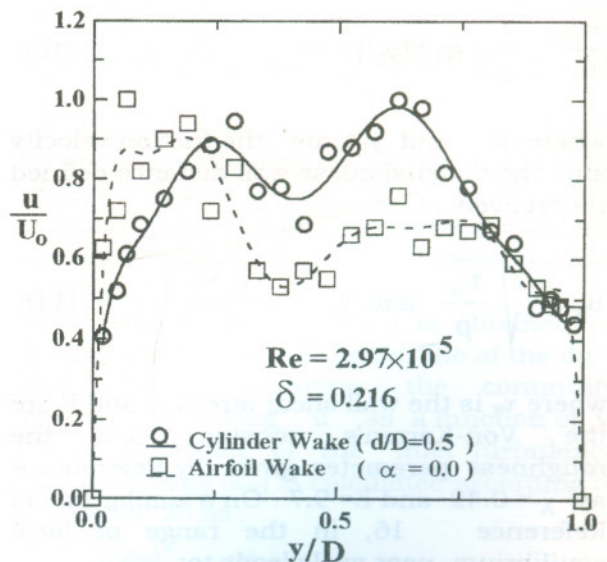

Figure 3 Measured wake velocity profiles at entrance of the curved duct

Let the wake half-width (b) be the value of y at which the velocity defect equals half of its maximum value. It is noticed that, the half-width of the generated wake is not the same on the two sides of the wake. The

velocity defect (w) at a radial station can be defined as the difference between the velocities at that point without the wake and with the wake. The procedure for determining the velocity defect distribution is described in details by Schobeiri et al. [13]. The mean velocity defect and its maximum value at the wake center are calculated as follows. A hypothetical velocity distribution is determined in the wake by fitting the mean velocity data outside the wake on both halves by a suitable curve. Nakayama [11] used a straight fit to obtain the hypothetical potential velocity distribution. This method is used also in the present study. The measured inlet velocity profile after the wake generator was used in the calculation for comparison purpose. From the comparison of the two-wake velocity profiles, it can be noticed that, the minimum velocity in the airfoil wake is smaller than that in the case of a cylinder wake. As a consequence, the dimensionless maximum velocity defect (w_o=0.26) behind the airfoil is greater than that generated by the cylinder (w_o =0.18). The main reasons of this observation can be explained as follows. For the case of using the airfoil as a wake generator, flow takes place around airfoil, the boundary layer separates from the surface towards the rear of the airfoil. Downstream of the separation position, the flow is greatly disturbed by large scale-eddies, and this region of eddy motion is usually known as the wake. As a result of the energy dissipated by the high intensity vortices in the wake, the pressure there is reduced and the entrainment rate of external flow to the wake region is increased. At zero-incidence angle, separation occurs over NACA-0012 airfoil towards the trailing edge and the wake is weak. Therefore, the rate of entrainment is small compared to that in the case of a wake behind a cylinder, which causes a faster separated flow and the wake is wider. As a result, the minimum velocity in the wake behind a cylinder is greater than that produced by the airfoil. In addition, the presence of tripping wire on the leading edge of the airfoil causes an increase in the

distortion or velocity defect in the axial velocity profile compared with the corresponding value for the smooth cylinder.

Static Pressure Distributions

The influence of the variation of the wake strength on the wall static pressure coefficient, C_p, along the inner and outer walls of bends will be discussed in this section. The wall static pressure coefficient C_p is defined as $C_p = (P - P_{ref}) / (0.5 \rho U^2_o)$, where P_{ref} is the reference wall static pressure at z / D=5 upstream the wake generator. The strength of the wake generated behind a cylinder was varied by using cylinders with different diameters, namely d/D = 0.1, 0.3 and 0.5. While the strength of the wake generated behind an airfoil was changed through the variation of the airfoil setting angle (α), namely α=0, 15 and 30 degrees. Measurements of static pressure distributions were conducted for two 90 degrees bends with curvature ratios of 0.216 and 0.368 at different Reynolds numbers. Selected samples of the results are plotted in Figures 4 to 11. Included in these figures are results for static pressure distribution without the wake generator. With respect to the wake generated behind the cylinder, Figures 4 to 7, all the pressure distributions for both bends have following the same general characteristics. Variation of the pressure distribution start to occur in the upstream tangent. Adverse pressure gradients develop on the outer walls of the bends and favorable gradients are formed on the inner walls. At certain angle inside the bend, the pressure distribution on the outer wall becomes favorable, whereas an adverse pressure gradient is formed on the inner wall. When the cylinder wake was imparted to the flow at the bend entrance of curvature ratio of 0.216, the pressure distribution along the outer wall almost decreases and the C_p values become lower than those in the case of no-cylinder wake, Figure 4. Increasing the cylinder diameter reduces the pressure coefficient along the outer wall of the bend owing to increasing the additional losses in the wake region behind the cylinder. However, the pressure distribution

along the inner wall of the same bend (δ = 0.216) appears to be less sensitive to the variation of wake strength. This may be due to the strong effect of streamline curvature. It is well known that, the presence of curved duct influences the wall pressure variations even at one diameter upstream of the curved duct entrance and abrupt changes in the static pressures on the convex and the concave walls take place before and after the curved duct. Similar changes can be found in other experiments, e. g. So and Mellor [22], [23] and Ellis and Joubert [24]. However, the presence of wake flow inside the curved duct strongly influences the pressure distribution for a larger upstream distance than that in the case of no-wake flow. This is due to that, the primary effect of these wake generators is to lower the static

pressure coefficient in the region of the wake generator due to the decreased effective flow area. There has also been a slight loss in pressure coefficient due to the wake generator loss.

In general, the curvature ratio (δ= $D/2R_c$) determines the pressure difference between the inner and outer walls. For the bend of curvature ratio of 0.368, Figures 6 and 7, and in the absence of wake flow, it can be observed that the streamwise pressure distributions are strongly adverse on the outer walls of the bend up to 75 degrees and strongly adverse on the inner wall up to the same location inside the downstream tangent (z/D = 2.1). The presence of an adverse pressure gradient on both walls may causes flow separation inside the bend and hence more pressure losses will be yielded.
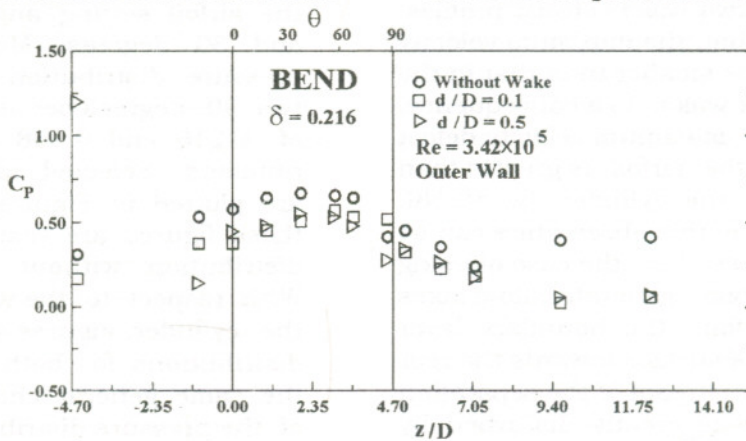
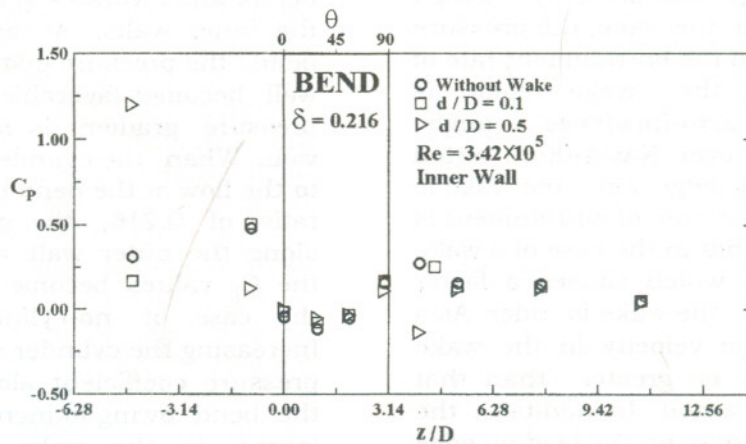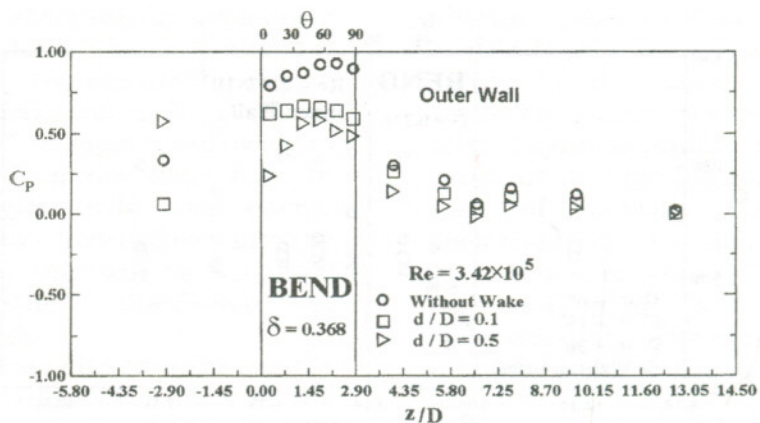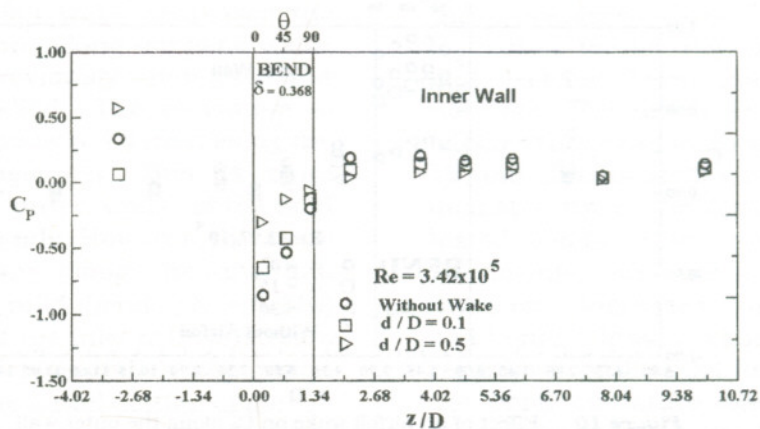**Figure 4** Effect of a cylinder wake on C_p along the outer wall

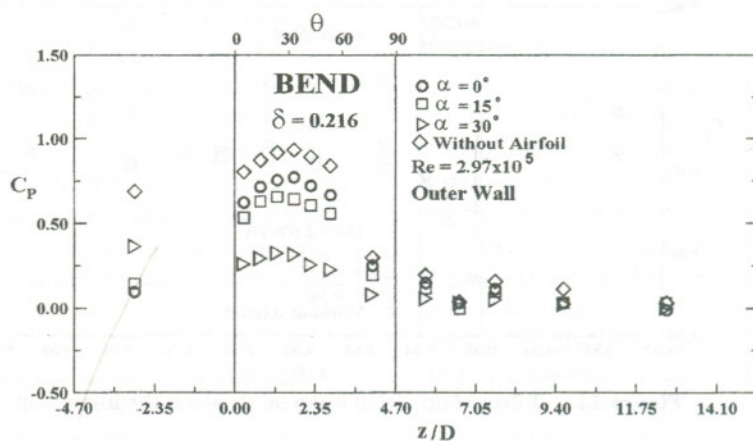**Figure 5** Effect of a cylinder wake on C_p along the inner wall

Figure 6   Effect of a cylinder wake on C_P along the outer wall

Figure 7   Effect of a cylinder wake on C_P along the inner wall

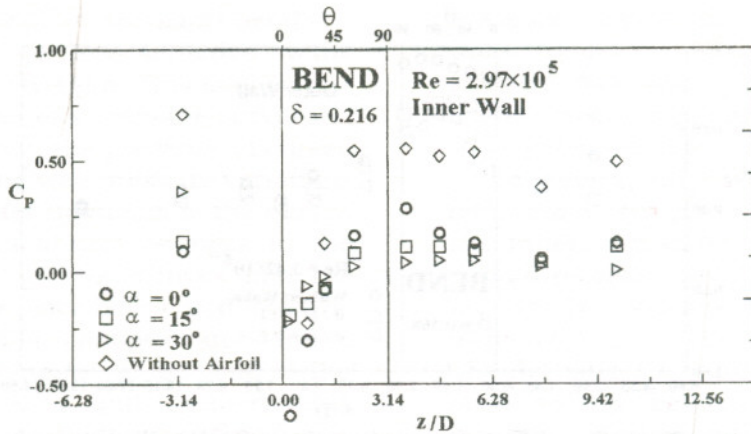**Figure 8**   Effect of an airfoil wake on C_P along the outer wall

Figure 9   Effect of an airfoil wake on C_P along the inner wall
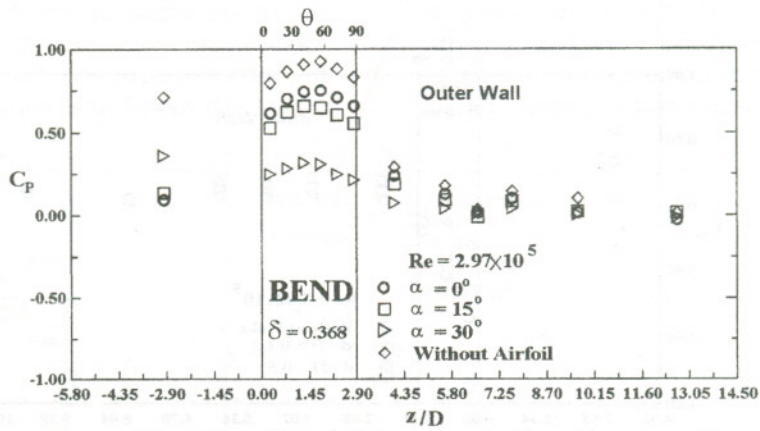

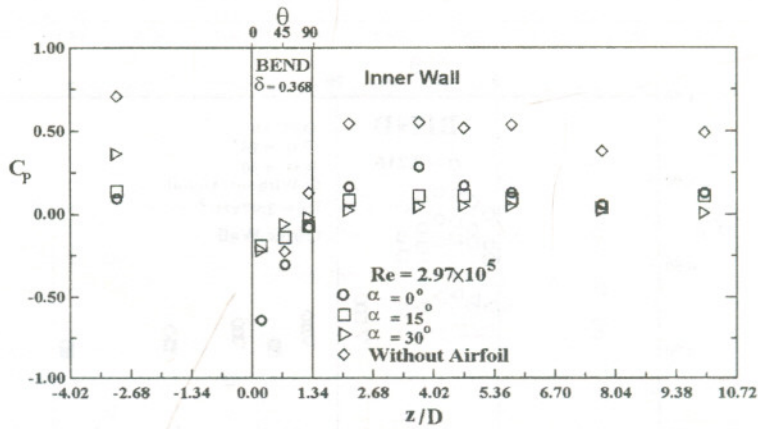**Figure 10**   Effect of an airfoil wake on C_P along the outer wall

Figure 11   Effect of an airfoil wake on C_P along the inner wall

According to the results of cylinder wake flow in the sharp radius bend, as shown in Figures 6 and 7, presence of wake flow relaxes the pressure inside the bend. Along the outer wall of the bend, the largest decrease in the streamwise pressure coefficient is noticed when cylinder diameter ratio of 0.5 is installed upstream the bend entrance. Therefore, it can be concluded that the flow separation inside the sharp

bends is controlled effectively by installing a cylinder with a suitable diameter ahead of the bend entrance. The separation control, mainly, may be attributed to the growth of the boundary layer is suppressed owing to the velocity defect of the wake flow. In addition, the higher turbulence energy produced by the wake flow diffuses into the boundary layer and this will be discussed latter during the discussion of computational results.

The influence of the curved wake created by a symmetrical airfoil NACA-0012 on the bend performance, is shown at Figures 8 to 11. The static pressure distributions for both bends indicate clearly that, the introduction of airfoil wake decreases the pressure distribution along the bend walls; this is obtained previously when a circular cylinder was installed. The relaxation of static pressure increases by increasing the airfoil setting angle (α). This is more remarkable on the outer walls of the mild and sharp radius bends. However, the static pressure distributions along the inner and outer walls of the mild bend (δ = 0.216) have flat regions at the inlet of downstream tangent, which represented a separation tendency, when the airfoil setting angle α = 30 degrees, see Figures 8 and 9. This occurs due to the separation and reverse region formed over the airfoil when the setting angle becomes more than the critical airfoil stalling angle (α= 10 degrees) [21]. On the other hand, no flat regions are observed in pressure distribution in the case of the sharp radius bend (δ = 0.368), as shown in Figures 10 and 11. This may be due to the strong interaction between the streamline curvature and the generated wake which results in a high intensity of secondary flow inside the bend [12].

Streamwise Pressure Loss Coefficient

The variation of the bend loss coefficient (k_b) of mild and sharp radius bends as a function of Reynolds number with and without wake are presented in Figures 12 to 15. The streamwise pressure loss coefficient is defined as k_b = $\Delta p / 0.5 \rho U^2_o$, where Δp is the streamwise pressure drop between entrance and exit of the bend. In the case of a mild bend (δ =0.216) with a cylinder wake, Figure 12, it is shown that the bend loss coefficient decreases with increasing the inlet Reynolds number and becomes almost constant at high Reynolds numbers. In the case of no-wake flow, the bend loss coefficient of the sharp radius bend (δ =0.368) decreases as the Reynolds number increases up to R_e = 2.33 x 10^5 and then increases with increasing the inlet Reynolds number owing to the presence of separation and a strong swirling secondary flow arising from the centripetal acceleration, see Figure 13. When a cylinder with diameter ratio of d/D = 0.1 is installed upstream the bend, the pressure loss coefficient almost decreases for all Reynolds number values and becomes lower than that in the case of no-wake. The diameter of the cylinder also affects the pressure loss coefficient. Figures 12 and 13 indicate the effects of the cylinder diameter upon the loss coefficient for both tested bends. It is observed that, the loss coefficients are increased as the cylinder diameter increases on account of an additional losses caused by the wake, regardless of the inlet Reynolds number and the bend curvature ratio. Therefore, it can be concluded that the bend loss coefficient strongly depends on the velocity defect in the axial velocity profile at the bend entrance.

As discussed above, it is clear that the presence of a cylinder with a suitable diameter is useful for improving the bend performance, especially for bends with large curvature ratios. The effect of wake generator type, also, affects the bend performance. Figures 14 and 15 show the variation of bend loss coefficient against the inlet Reynolds number in the presence of a wake behind NACA-0012 airfoil. The effect of the incidence angle (α) of the airfoil is also included in these figures. It is found that, the presence of an airfoil at zero-incidence angle yields the lowest loss coefficients for both tested bends within the test range of Reynolds number. Further increase in the incidence angle increases the streamwise loss coefficient values but still lower than

those with no-airfoil wake. This may be explained as follows. When the airfoil incidence angle increases at constant Reynolds number, the velocity defect increases due to the strong adverse pressure gradient and the streamline

curvature. Correspondingly, the decay of the wake through the bend is slower when the wake subjected to positive pressure gradient. This observation was confirmed previously by Schobeiri and John [14].
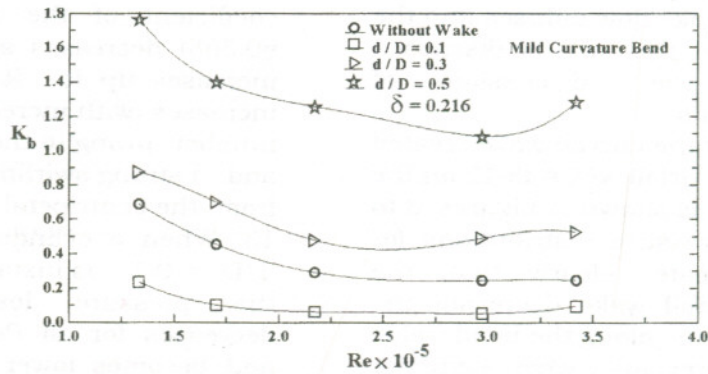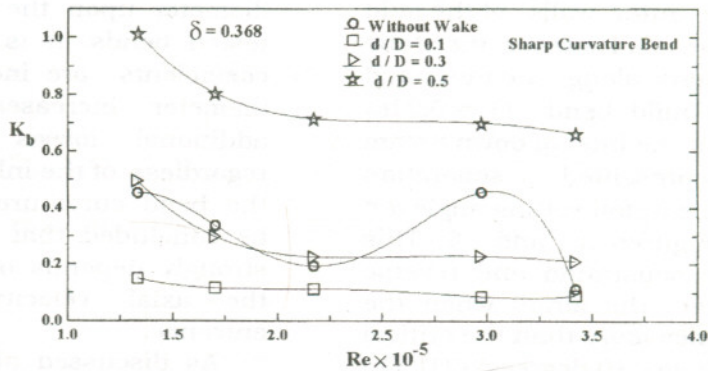

Figure 12   Effect of a cylinder wake on streamwise pressure loss coefficient

Figure 13   Effect of a cylinder wake on streamwise pressure loss coefficient
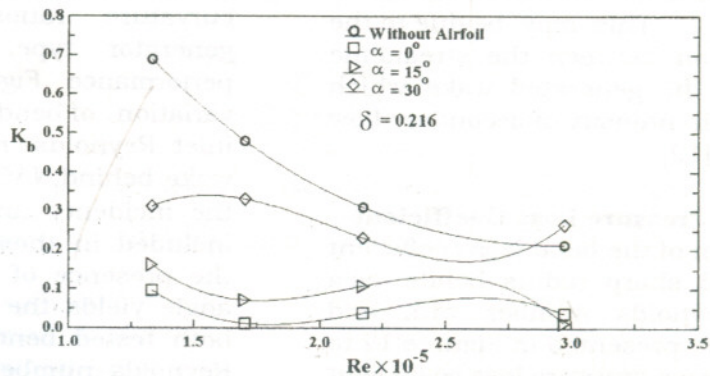

Figure 14   Effect of an airfoil wake on streamwise pressure loss coefficient
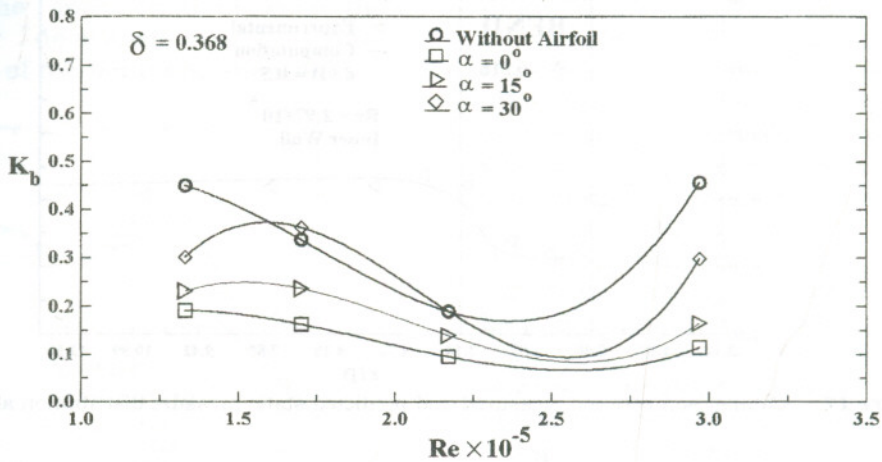
Figure 15   Effect of an airfoil wake on streamwise pressure loss coefficient

THEORETICAL RESULTS AND VERIFICATION

To verify the numerical method, samples of predicted static pressure distributions are compared with the experimental results obtained for a mild curved bend (δ =0.216). The comparison is shown in Figures 16 to 19. Computations and measurements were performed for inlet Reynolds number of 2.79×10^5 in the presence of wake flows. In general, good agreement between predicted and measured values of static pressure distributions are obtained.
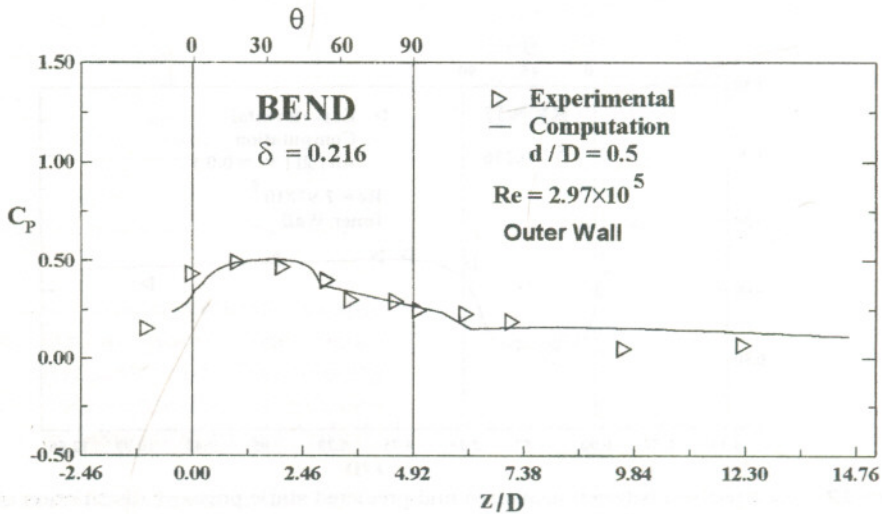

Figure 16   Comparison between measured and predicted static pressure distribution along outer wall
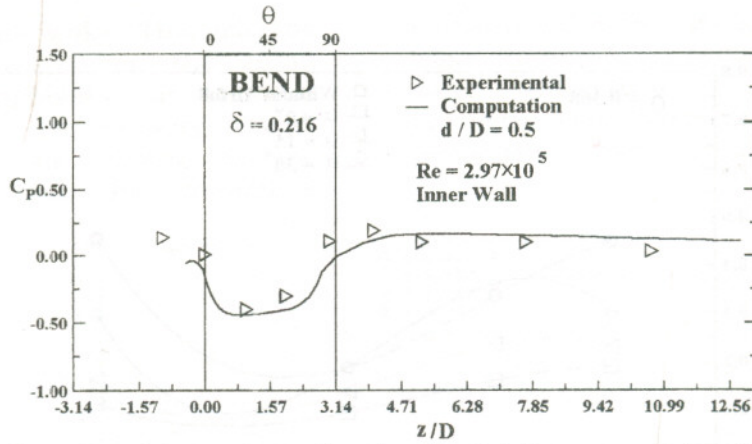
Figure 17   Comparison between measured and predicted static pressure distribution along inner wall

Figure 18   Comparison between measured and predicted static pressure distribution along outer wall

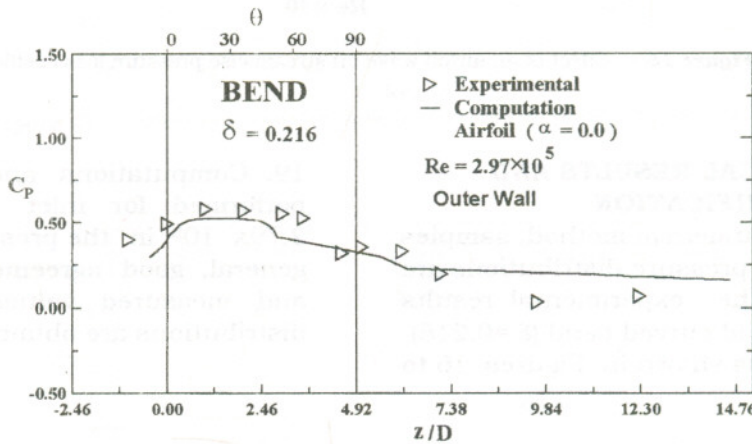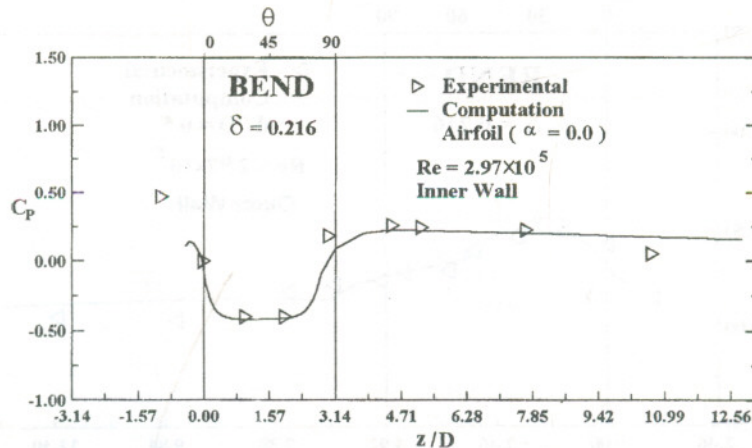**Figure 19**   Comparison between measured and predicted static pressure distribution along inner wall

The predicted distributions of the mean velocity profiles in the presence of cylinder wake and airfoil wake are illustrated in Figures 20 and 21, respectively, at different locations inside the bend ($\delta = 0.216$). The calculations are performed based on the measured inlet velocity profiles which are fitted and denoted by solid lines in the

figures. From these figures, it can be seen clearly that the interaction between the boundary layer developed over the inner and outer sides of the bend and the wake.
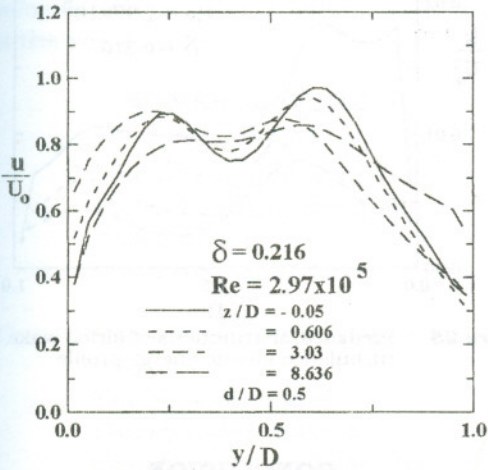

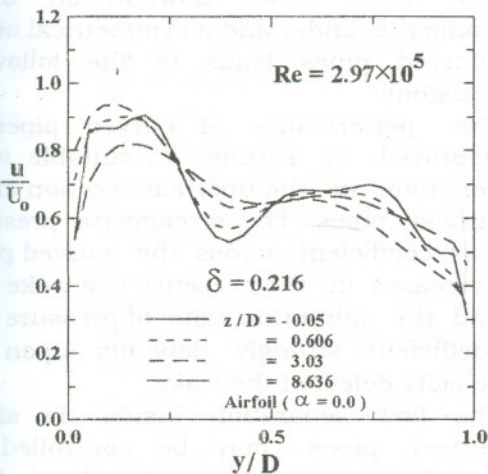**Figure 20** Predicted distributions of a cylinder wake mean velocity profile

Figure 21 Predicted distributions of airfoil wake mean velocity profile

In general, the mean velocity profile becomes asymmetrical about the wake centerline. The asymmetry in the velocity profile about the wake centerline is reduced with an increase in axial distance form the bend entrance.

As the wake convects through the bend, the wake center gradually moves towards the bend center. The maximum wake velocity defect (w_o) for either cylinder wake or airfoil wake decreases, as shown in Figure 22, resulting in a continuous

increase in the wake width (b) with downstream direction, as shown in Figure 23, because of the diffusional processes that take place in turbulent shear layer. On the other hand, the strongest asymmetry is seen in the case of wake behind airfoil and the velocity profile did not recover uniformity at the bend exit. However, the wake behind the cylinder starts to recover uniformity near to the bend exit. This is due to the pressure variation across the wake. For a wake behind cylinder, it is seen from Figure 20 that, the wake is subjected to a small adverse pressure gradient at the bend entrance, which is measured by the difference between velocities at the upper and lower edges of the wake. In the case of the wake behind the airfoil, the wake is subjected to strong adverse pressure gradient at the bend entrance owing to the difference in velocities at the wake edges which is higher than that in the case of cylinder wake, (Figure 21). Thus, the relaxation of pressure gradient and curvature are slower as the wake convects through the bend. Based on this explanation, Figure 22 indicates that the decay of the velocity defect is faster at small pressure gradient (cylinder wake) than that at a strong pressure gradient (airfoil wake). Conversely, the growth of the wake width is faster at strong pressure gradient than that occurs at a small pressure gradient, as shown in Figure 23.
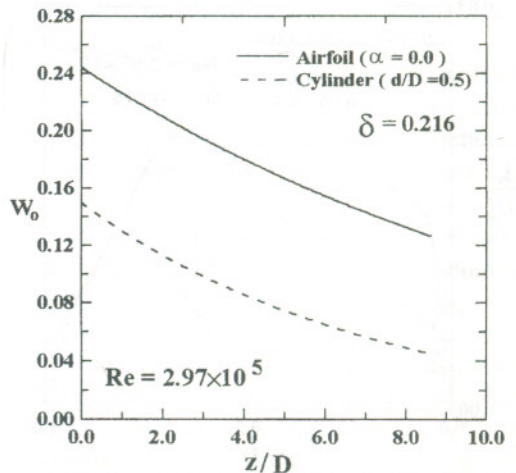

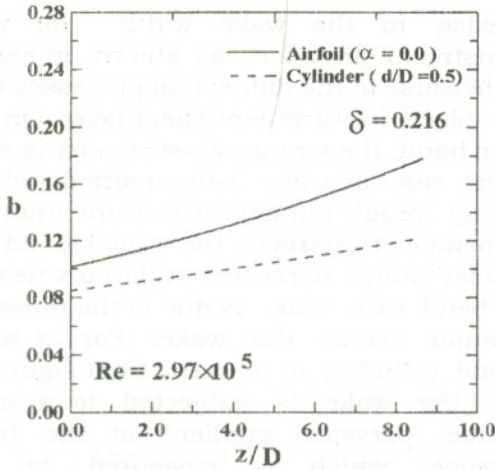**Figure 22** Variation of maximum wake defect

Figure 23 Variation of wake half-width

Figure 25 Predicted distributions of airfoil wake turbulence kinetic energy profile

The distributions of the turbulence kinetic energy at various longitudinal locations are presented in Figures 24 and 25 for cylinder wake and airfoil wake, respectively. As shown in these figures, the turbulence level increases in the boundary layer and in the wake region with increasing the degree of asymmetry of the velocity profile, owing to the curvature effect that causes a pressure gradient resulting in a highly asymmetric distribution of turbulence kinetic energy. As the flow proceeds downstream, the high turbulence energy in the wake region diffuses over the whole flow region which may suppress the boundary layer growth and hence the flow separation may be controlled.
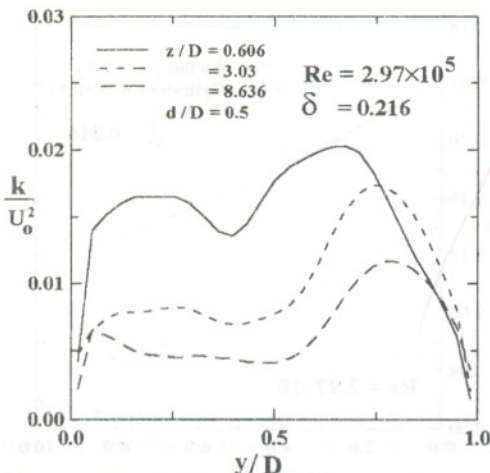

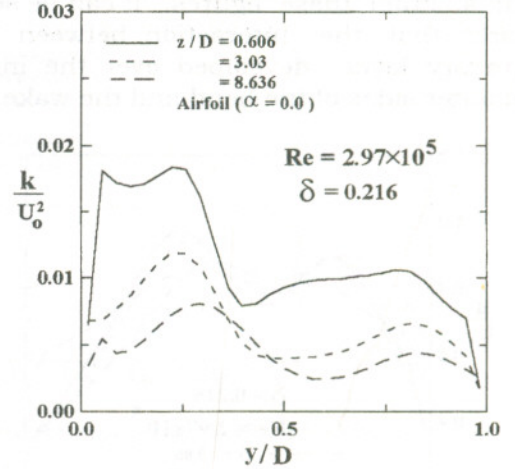**Figure 24** Predicted distributions of a cylinder wake turbulence kinetic energy profile

CONCLUSION

The investigation on the development of steady wake flows downstream of a stationary cylinder and a symmetrical airfoil in curved pipes leads to the following conclusions:

1. The performance of curved pipes is improved by setting a suitable wake generator in the upstream section of the curved pipes. The streamwise pressure loss coefficient across the curved pipes decreases in the presence of a wake flow and the minimum value of pressure loss coefficient strongly depends upon the velocity defect of the wake.

2. The flow separation inside the sharp curved pipes may be controlled by installing a wake generator ahead of the curved pipe owing to the velocity defect of the wake and the higher turbulent energy by the wake flow.

. Mean velocity profiles are observed to be asymmetrical about the wake centerline when the wake is influenced by the pressure gradient and curvature.

4. The turbulence level increases in the boundary layer and in the wake region with increasing the degree of asymmetry of the velocity profile.

The maximum wake velocity defect decreases and the wake width increases as the wake convects through the curved pipe. The presence of a wake in a pressure gradient delays the decay of the velocity defect and increases the growth of the wake width.

NOMENCLATURE

b	The half-wake width.
$\bar{b}$	The average value of b on the walls of curved duct
c	Airfoil chord
C_p	Pressure coefficient
$C_D, C_1,$	
C_2, C_μ	Constants in turbulence model
D	The pipe diameter
d	The cylinder diameter
E	Constant depends on the wall roughness
G	Generation of turbulence kinetic energy
k	Turbulence kinetic energy
K_b	Streamwise pressure loss coefficient
P	Static pressure.
P_{ref}	Reference pressure
Rc	Mean curvature radius
Re	Reynolds number based on the inlet conditions
U_o	Inlet mean velocity
u, v	Axial and normal velocities
w	wake velocity defect
w_o	Maximum wake-velocity defect
z, y	Streamwise and normal coordinates

Greek symbols

α	Airfoil setting angle
Γ_Φ	Effective diffusivity for Φ
δ	Curvature ratio
θ	Angular position
Φ	Dependent variable
μ_{eff}	Effective viscosity
μ_ℓ	Laminar viscosity
μ_t	Turbulent viscosity
ρ	Fluid density

REFERENCES

1. H. Ito, "Flow in Curved Pipes" JSME International J., Vol. 30, pp. 543, (1987).

2. S.A. Berger, S.A. Talbot and L.S. Yao, "Flow in Curved Pipes", Annual Review of Fluid Mech., Vol. 15, pp. 461, (1983).

3. H. A. Abdalla, M. Naser, B.A. Khalifa and W.A. El-Askary, "Effects of Geometrical Parameters and Inlet Conditions on Turbulent Flow Structures and Performance of 90°-Bend", Alexandria Engineering J., Vol. 36, No. 1, pp. A1, (1997).

4. H. Schlichting, "Boundary layer Theory", Sixth edition, McGraw-Hill, (1968).

5. A.A. Townsend, "The structure of Turbulent Shear Flow". Cambridge, University Press, England, (1976).

6. K.R. Sreenivasan and R. Narasimha, "Equilibrium parameters for two-dimensional turbulent wakes", ASME, J. Fluid Engineering, Vol. 104, pp. 167, (1982).

7. I. Wygnanski, F. Champagne and B. Marasli, "On the large-scale structures in two-dimensional, small deficit, turbulent wakes", J. Fluid Mech., Vol. 168, pp. 31, (1986).

8. S. Gartshore, Ian, "Two-Dimensional Turbulent Wakes", J. Fluid Mech., Vol. 30, Part 3, pp. 547, (1967).

9. R. Raj and B. Lakshminarayana, "Characteristics of the wake behind a cascade of airfoils", J. Fluid Mech., Vol. 81, Part 4, pp. 707, (1973).

10. A.M. Savil, "The Turbulent Structure of a Highly Curved Two-Dimensional Wake", Proc. on Complex Turbulent Flows, Springer, New York, pp. 185, (1983).

11. A. Nakayama, "Curvature and Pressure gradient effects on a small defect wake", J. Fluid Mech., Vol. 175, pp. 215, (1987).

12. V. Ramjee, E.G. Tulapurkara, and R. Rajasekar, "Development of Airfoil Wake in a Longitudinally Curved Stream", AIAA J., Vol. 26, pp. 948, (1988).

13 M.T. Schobeiri, K. Pappu, and J. John, "Theoretical and Experimental study of Development of Two-Dimensional Steady and unsteady wakes within Curved Channels", ASME, J. Fluids Engineering, Vol. 117, pp. 593, (1995).

14. M.T. Schobeiri and J. John, "Development of a Two-Dimensional Turbulent Wake in a Curved Channel with a Positive Streamwise Pressure Gradient", ASME, J. Fluids Engineering, Vol. 118, pp. 292, (1996).

15. S.V. Patankar, V.S. Pratap and D.B. Spalding, "Prediction of Turbulent Flow in Curved Pipes", J. Fluid Mech., Vol. 67, pp. 583, (1975).

16. B.E. Launder and D.B. Spalding, "The Numerical Computation of Turbulent Flows", Computer Methods in Applied Mechanics and Engineering., Vol. 3, pp. 269, (1974).

17. R. Houdeville and E.G. Tulapurkara, "Prediction of Boundary Layers, Wakes and Mixed Flows Using Modified k-ε Model", ONERA CERT Report Technique OA 46/2259, (1981).

18. M.A. Leschziner and W. Rodi, "Calculation of Annular and Twin Parallel Jets Using Various Discretization Schemes and Turbulence Model Variations", Trans. ASME, J. Fluids Engg., Vol. 103, pp. 352, (1981).

19. A.D. Gosman, and W.M. Pun, "Calculation of Recirculating Flows", Rept. No. HTS/74/12, Dept. of Mech. Engg., Imperial College, London, England, (1974).

20. B.R. Ramaprian, V.C. Patel and M.S. Sastry, "The Symmetric Turbulent Wake of Flat Plate", AIAA J., Vol. 20, pp. 1228, (1982).

21 I.H. Abott, A.E. Von Doeuhoff, "Theory of Wing Sections", Dover Publications, (1959).

22. R.M.C. So and G.L. Mellor, "Experiments on Convex Curvature Effects in Turbulent Boundary Layers", J. Fluid Mech., Vol. 60, pp. 43, (1973).

3. R.M.C. So and G.L. Mellor, "Experiments on Turbulent Boundary Layers on a Concave Walls", Aero. Q. , Vol. 26, pp. 25, (1975).

24 L.B. Ellis and P.N. Joubert, "Turbulent Shear Flow in a Curved Duct", J. Fluid Mech. , Vol. 62, pp. 65, (1974).

دراسة أثر مخر السريان الإضطرابى فى الأنابيب المقوسة

حسن عوض محمد عبد اللـــه

قسم هندسة القوى الميكانيكية – جامعة المنوفية

ملخص البحث

فى هذا البحث ، تم دراسة أثر مخر السريان الإضطرابى فى الأنابيب المقوسة – تم توليد المخر فى السريان الإضطـرابى عنـد مدخل الأنابيب المقوسة بوضع إسطوانات رأسية ذات مقطع دائرى بأقطار مختلفة – كما تم توليد المخر باستخدام جسم ذو مقطع إنسيابى (إيروفيل) عند زوايا هجوم مختلفة. لدراسة تأثير التقوس على تطور المخر وأثره على السريان الإضطرابى ، إستخدم فى الدراسة أنابيب بنسب تقوس مختلفة.

فى هذا البحث ، تم دراسة أثر المخر على السريان الإضطرابى فى الأنابيب المقوسة معمليا ونظريا ، شملت الدراسة المعمليــة قياس توزيع السرعة خلف مولد المخر ، توزيع الضغط الإستاتيكى على السطح المقوس الداخلى والسطح الخـارجى للأنابيب وكذلك معامل الفقد للضغط . أجريت القياسات مع تغيير رقم الرينولدز عند الدخول ونسبة التقوس . أوضحـت القياسـات المعملية أن معامل الفقد للضغط فى الأنابيب المقوسة يعتمد على خصائص المخر عند المدخل (مثل العرض – العمق وشدة المخر) و نسبة التقوس ورقم الرينولدز عند المدخل .

تمت الدراسة النظرية لأثر المخر على خصائص السريان الإضطرابى فى الأنابيب المقوسة بحل المعادلات الحاكمة للسريان مـع نموذج الإضطرابات الذى يشتمل على تأثير التقوس . أظهرت المقارنة بين النتائج النظرية والمعملية تقاربـا مقبـولا وأن نمـوذج الإضطرابات يمكن إستخدامه لدراسة هذا النوع من السريان – كذلك أوضحت الدراسة النظرية والقياسات المعملية عدم تماثل توزيع السرعة حول محور المخر نظرا لتأثير كل من التقوس والضغط على السريان .